ELSEVIER

Contents lists available at ScienceDirect

Construction and Building Materials

journal homepage: www.elsevier.com/locate/conbuildmat





Evaluation of the bonding properties between low-value plastic fibers treated with microbially-induced calcium carbonate precipitation and cement mortar

Michael Espinal a,b, Seth Kane a,b, Cecily Ryan a,b, Adrienne Phillips b,c, Chelsea Heveran a,b,*

- ^a Mechanical and Industrial Engineering Department, Montana State University, Bozeman, MT 59717, USA
- ^b Center for Biofilm Engineering, Montana State University, Bozeman, MT 59717, USA
- ^c Civil Engineering Department, Montana State University, Bozeman, MT 59717, USA

ARTICLE INFO

Keywords: Biomineralization Microbially-induced calcium carbonate precipitation Fiber-reinforced mortar Bond strength Waste plastic

ABSTRACT

Plastic fiber reinforced cementitious materials offer the potential to increase the reusability of plastic waste and create lower-CO₂ cementitious composites. However, the bonding properties of many plastic types with ordinary Portland cement (OPC) are largely unknown. This work employs single fiber pullout (SFPO) tests to quantify the interfacial bonding properties of polyvinyl chloride, low-density polyethylene, polypropylene, polystyrene, and acrylonitrile butadiene styrene embedded in OPC mortar. The interfacial bonding properties were compared for fibers either treated with microbially-induced calcium carbonate precipitation (MICP) or left untreated. SFPO tests revealed that plastic type had a large influence over bonding properties. Specifically, the fiber surface energy, as estimated from water contact angle measurements, was found to be the driving factor of bond strength. ABS had the highest surface energy and demonstrated the strongest bonding out of all plastic types studied. However, MICP treatment of fibers did not increase the interfacial bond strength for any of the plastics studied. The thick and inconsistent coverage of biomineral over the fiber surface from MICP is likely attributed to preventing an increase in bond strength. These results contribute to the design and application of plastic-reinforced mortars by comparing bonding properties for a range of typically low-value, unrecycled plastic types.

1. Introduction

Ignited by the threat of climate change, researchers have been developing ways to reduce the carbon dioxide (CO_2) emissions from the production of concrete. Production of ordinary Portland cement (OPC), the binding material in standard concrete, is responsible for between 5 and 8% of anthropogenic global CO_2 emissions [1,2]. A promising strategy towards mitigating these impacts is to replace a portion of the OPC with a waste or low carbon footprint material.

To date, most partial replacements of OPC are from industry by-products, such as fly ash and blast furnace slag [1,3]. Waste plastics are another candidate to replace a portion of OPC, since plastic fibers can serve as a reinforcing material [3]. Polyvinyl chloride (PVC, type 3), low-density polyethylene (LDPE, type 4), polypropylene (PP, type 5), polystyrene (PS, type 6), and acrylonitrile butadiene styrene (ABS, type 7) may be candidates for waste plastics in fiber-reinforced cementitious

materials. Currently, these low-value, challenging-to-recycle plastics are typically landfilled, incinerated, or accumulate in the environment [4,5]. When utilized in cementitious composites, plastic waste is typically added as a pure reinforcement (i.e., does not reduce the amount of OPC binder) [6–8] or replacement of aggregate [9–15]. While these additions of plastics succeed at repurposing plastic waste, a partial replacement of the OPC with plastic has the potential to further improve the sustainability of the cementitious material [16].

A challenge with the incorporation of plastic fibers into cementitious materials is that their usage decreases the compressive strength of the composite [12-15,17-19]. Previous efforts with using plastic as a reinforcement have utilized very small additions of plastic (e.g., < 2%) [6,17]. When greater additions are used, larger decreases in strength are seen [12-15,17,18]. For instance, Wang et al. [15] showed that including recycled high impact polystyrene at a 50% volume replacement of sand led to a 49% reduction in strength compared to a 12%

E-mail addresses: michael.espinal@student.montana.edu (M. Espinal), sethkane@montana.edu (S. Kane), cecily.ryan@montana.edu (C. Ryan), adrienne. phillips@montana.edu (A. Phillips), chelsea.heveran@montana.edu (C. Heveran).

^{*} Corresponding author.

strength reduction at a 10% replacement of sand in cement mortars. The reason for the reduction in strength with the addition of recycled plastic can be attributed to poor interfacial bonding between the plastic and cement [18]. Several surface treatments have been evaluated for their potential to increase the bond between the plastic surface and mortar. These include chemical [20–23], mechanical [21,24], plasma [25–29], and particle (biochar [8], silica [30–32], SiO₂ [33], calcium carbonate [16,34,35]) surface treatments.

Calcium carbonate (CaCO₃) surface treatments stand out among other possible fiber treatments due to the demonstrated ability of CaCO₃ to repair cracks in concrete and seal leaky oil wells [36,37]. The ability of CaCO3 to bond to the cement matrix, such as is required for sealing cracks, suggests that CaCO3 could improve the interfacial bond between plastics and cement, thereby strengthening the overall composite. In a previous research effort, Kane et al. utilized microbially-induced calcium carbonate precipitation (MICP) to deposit a CaCO3 biomineral coating on plastic fibers. The treated fibers were then incorporated as a partial cement binder replacement (1-5 wt%) into plastic-reinforced mortar (PRM) [16]. MICP treatment significantly increased the compressive strength of PRM containing PVC (18% increase) but had limited impact on other plastic types. It was also found that PRM with MICP treated mixed types 3-7 plastics had high compressive strength values (91% of the strength measured in mortar specimens containing no plastic) [16]. The benefit to compressive strength was greater for MICP than for enzyme-induced calcium carbonate precipitation using Jack Bean meal as the enzyme source, suggesting that the microbial precipitation promotes stronger fiber attachment to mortar [16]. However, the compressive strength of composites containing individual plastic types 4-6 was not improved by MICP treatment, further motivating the need to determine why MICP treatment improves composite strength for PRMs containing some plastics but not others.

Single fiber pullout (SFPO) tests can be used to compare the bond strength between different plastic types and cement and whether these bond strengths are improved by MICP treatment. Most prior PRM and plastic-reinforced concrete (PRC) studies have considered PP [8,20–23,31,32,34,35,38–41] or higher-value recyclable plastics such as polyethylene [26,27,42]. Hao et al. [34] used SFPO tests to identify that PP's bond strength with cement mortar can be enhanced with certain ratios of mineral weight per weight of fiber. However, there are important gaps in knowledge about how other common low-value waste plastics (e.g., LDPE, PVC, ABS) bind to cement and whether these bond strengths benefit from MICP treatment. Closing these gaps is crucial for optimizing PRM and PRC design as the interfacial bond strength influences their mechanical properties [43].

This study quantifies the interfacial bond strength, frictional bond strength, chemical bond energy, and work to pullout of low-value plastics type 3, 4, 5, and 7 with and without MICP treatment using SFPO testing. SFPO tests were also conducted on treated and untreated plastic type 6 fibers, however the bonding parameters were not quantified. Because a prior study by the authors determined that PRMs had different strengths depending on the type of low-value plastic utilized (i. e., LDPE and PVC lowest, ABS and PS highest for non-treated fibers) [16], it was hypothesized that bond strength would mirror these findings. It was further hypothesized that calcium carbonate (CaCO₃) biomineral from MICP would improve bonding between PVC and mortar, since PVC composites showed the greatest strength benefit from MICP in prior work [16].

2. Materials and methods

2.1. Plastic fibers

3D printer filament plastics were used to model common waste plastics. Polyvinyl chloride (PVC), linear low-density polyethylene (LDPE), polypropylene (PP), polystyrene (PS), and acrylonitrile butadiene styrene (ABS) were cut to 50 \pm 0.5 mm lengths for single fiber

pullout samples (Table 1). Fiber lengths were selected to ensure consistent embedment length between trials and because similar lengths have been used in prior SFPO studies [24,40,44]. The fibers were marked at 10 mm from the edge to act as a guide when manually embedding into mortar. Fiber density was derived from the mass of individual fibers and the volume. Fiber moduli were assessed through tensile testing using an Instron 5543. The loading rate was 5 mm/min and the distance between clamps was 30 mm.

2.2. Biomineralization of plastic fibers

2.2.1. Microorganism and culturing conditions

The bacteria culture was grown from a frozen stock of *S. pasteurii* (ATCC 11859) in 100 ml of growth media (37 g/L brain heart infusion broth and 20 g/L urea) following a previously established protocol [16]. The culture was grown in a shaking incubator at 150 RPM and 30 $^{\circ}$ C for 24 h. The parameters for the microbial solution followed those previously reported in Kane *et al.* [16].

2.2.2. Biomineralization of plastic fibers

Plastic fibers were coated with CaCO₃ biomineral via MICP. During MICP, the microbial urease of the *S. pasteurii* bacteria promotes calcium carbonate precipitation through urea hydrolysis [37]. The biomineralization media consisted of 8 ml of *S. pasteurii* culture per 400 ml of calcium mineralization media (3 g/L nutrient broth, 10 g/L ammonium chloride, 20 g/L urea, and 49 g/L calcium chloride dihydrate) [16]. The *S. pasteurii* inoculum and calcium mineralizing media were combined and stirred at approximately 400 RPM at room temperature. Biomineralization began when the group of 13 fibers were submerged in the biomineralization media for 48 h using a mesh bag (EcoWear-Amazon) (Fig. S1). Thirteen plastic fibers were mineralized per batch. The weight of each group of plastic fibers was recorded before and after biomineralization, following the drying of fibers overnight at room temperature. The weight was then divided by 13 to calculate the mean biomineral accumulated per fiber (Table S1).

2.3. Fiber embedment in OPC mortar

The mortar consisted of ordinary Portland cement (OPC) type I/II (Quickrete), water, and ASTM c778 graded sand as fine aggregate (U.S. Silica Company). Water:cement and sand:cement mass ratios were 0.46 and 0.80, respectively.

OPC cement and water were mixed in a kitchenAide mixer on slow speed for 30 s followed by another 30 s after adding the sand. The mortar was then mixed for 30 s on medium speed followed by a rest period where the mixer was turned off for 90 s. During the first 15 s of this break, the mortar stuck to the sides was scraped down into the bulk mortar. The mixer was then turned on for a final 60 s on medium speed. The mixing protocol follows ASTM C305 [45].

After mixing, $2'' \times 1'$ 4" film canisters (Houseables-Amazon) molds

Table 1 Properties of the plastic fibers. Measurements reported in mean \pm standard deviation. Fiber diameter was 1.75 mm for all plastic types.

| Plastic Type | Plastic Number | Manufacturer Name | Modulus (GPa) | Density (g/cm³) |
|-----------------|-------------------|-------------------------------------|-------------------|--------------------|
| PVC | 3 | Filamentum Vinyl 303 PVC – Black | 1.29 ± 0.19 | 1.35 ± 0.02 |
| LDPE | 4 | LLDPE108 Filament – Natural | 0.19 $0.16 \pm$ | 0.02 0.94 ± |
| | | | 0.03 | 0.01 |
| PP | 5 | Centaur Polypropylene Filament - | 0.30 \pm | $0.89 \pm$ |
| | | White | 0.02 | 0.00 |
| PS | 6 | NefilaTek 100 % Recycled | $0.65 \pm$ | $1.03~\pm$ |
| | | HIPS109 Filament – Black | 0.24 | 0.00 |
| ABS | 7 | NefilaTek 100 % Recycled ABS | 0.91 \pm | 1.04 \pm |
| | | Filament – Black | 0.27 | 0.01 |

were filled with mortar using a procedure adapted from ASTM C192 standard [46]. Before filling, a line was marked 7 mm below the top to ensure the mold caps were flush to the mold. Each mold was then filled half full of the fresh mortar. The mortar was tamped 25 times in a circular pattern (ensuring the inside the mold was evenly tamped) using a 10 mm rod and tapped around the bottom sides of the mold to remove air bubbles. The molds were then filled to the fill line and tamped again about half to three-quarters depth from the fill line to prevent air bubbles. The top of the mold was then tapped around the sides to release air bubbles.

After filling the molds, the fibers were embedded using a 3D printed mold cap to center the fiber during curing. Half of the mold cap was attached using tape to the top of the mold. The fiber was inserted through the center of the mold cap to the 10 mm mark followed by the placement of the second half of the cap. The samples were demolded after 24 h and cured for 7 or 28 days in a 70 $^{\circ}\mathrm{F}$ and 100% humidity curing chamber before single fiber pullout testing.

2.4. Biomineral coating characterization

2.4.1. Mineral texture and elemental composition

Samples of biomineralized fibers were imaged before and after SFPO testing using field emission scanning electron microscopy (FESEM, Zeiss Supra 55VP, 1 kV, working distance 4.7–6.6 mm). These samples were first sputter-coated with gold to improve conductivity.

The elemental composition of the biomineral coating was determined for additional biomineralized samples using energy dispersive X-ray spectroscopy (SEM-EDS) analysis (FESEM, Zeiss Supra 55VP, Oxford detector, 15 kV, working distance 8.5 mm). Samples studied with SEM-EDS were first coated with carbon.

2.4.2. Mineral identification

X-ray powder diffraction (Bruker D8 Advance Powder X-ray

Diffractometer) was used to characterize the crystalline structure of the ${\rm CaCO_3}$ biomineral precipitated on the fiber surface. The biomineral was scraped off the fiber surface 2 days after deposition and ground to a powder with mortar and pestle. MDI Jade was used to identify the diffractogram peaks.

2.4.3. Contact angle measurement

Video contact angle (VCA) measurements were acquired using a VCA 2500XE Video Contact Angle System. DI water droplets of size 4.0 \pm 0.5 μl were placed on the untreated plastic fiber surface. The mean VCA of each plastic is reported from five measurements per fiber. Contact angles less than 90° were considered hydrophilic while angles greater than 90° were considered hydrophobic.

2.5. Single fiber pullout tests

2.5.1. Instrumentation

Single-fiber pullout (SFPO) tests were performed using an Instron 5543 with a 1 kN load cell (Fig. 1). Aluminum base plates were milled to $150.0 \times 76.2 \times 19.05$ mm. Samples were centered on the plate and adhered with CrystalbondTM 509–1 adhesive. The base plate was heated on a hot plate at 200 °C to melt the adhesive. The samples were cooled at room temperature for a minimum 45–60 min before testing.

2.5.2. Single-fiber pullout testing and analysis

The minimum free length of the fiber was 4.5 mm. The tensile rate was 1 mm/min until the fiber was completely pulled out or snapped [30,34,40]. The pullout curves (load vs displacement) and fiber pullout properties were analyzed using MATLAB.

Pullout curves generated from SFPO tests were used to determine the interfacial bond strength (τ_a) , frictional bond strength (τ_b) , chemical bond energy (G_d) , and energy absorption (Fig. 2). Values for τ_a and τ_b were calculated based on the peak load (P_a) , Eq. (1)) and the load at

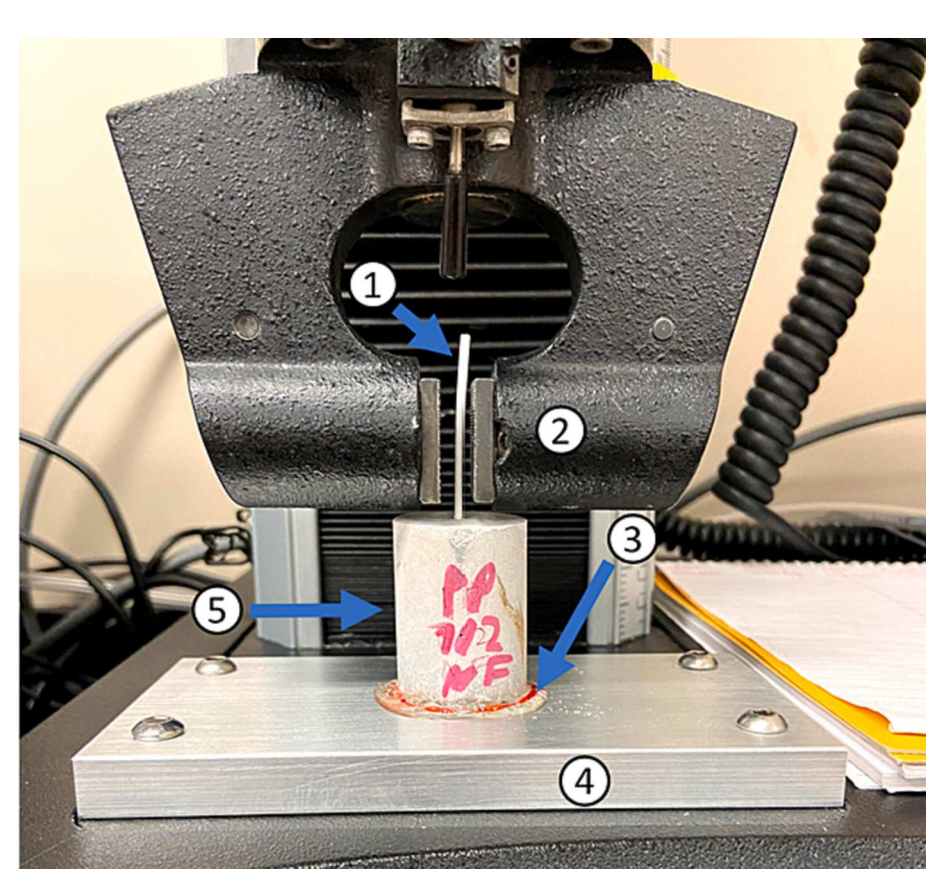
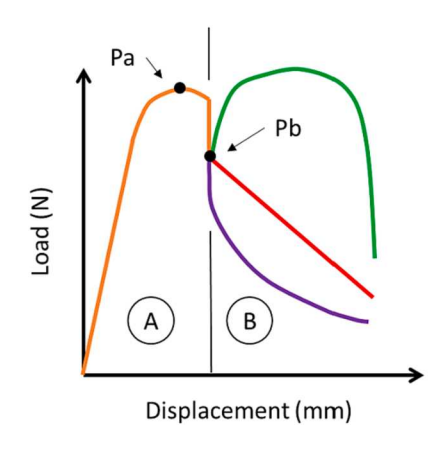


Fig. 1. SFPO testing arrangement. (1) Fiber, (2) Pneumatic grips, (3) Crystalbond adhesive, (4) base plate, (5) OPC cement mortar specimen.



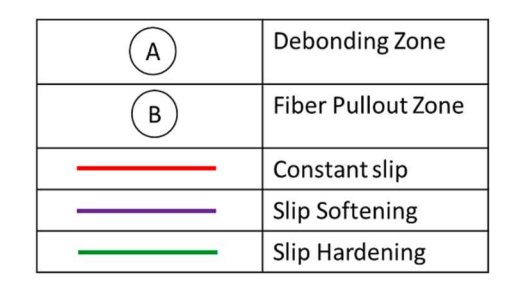


Fig. 2. A standard pullout curve generated from single fiber pullout tests showing the debonding (A), fiber pullout (B) regions and the three common frictional behaviors: constant slip, slip softening, and slip hardening.

which fiber pullout begins (P_b , Eq. (2)) and where l is the fiber embedded length, d is the fiber diameter, and E is the fiber modulus [35,40,47–49]. G_d was calculated using the load drop from P_a to P_b , signifying the broken chemical bond between the fiber and cement matrix (Eq. (3)) [35,48,49]. The energy absorbed (work) during SFPO tests was assessed from the area under the fiber pullout curve.

$$\tau_a = P_a/\pi dl \tag{1}$$

$$\tau_b = P_b/\pi dl \tag{2}$$

$$G_d = 2(P_a - P_b)^2 / \pi^2 E d^3 \tag{3}$$

The two regions of interest from the fiber pullout curves are the debonding region and fiber pullout region labeled as A and B respectively in Fig. 2. In the debonding region, the chemical and frictional bond breaks before the fiber begins to displace. The pullout region begins when the load drop from P_a to P_b occurs. The load–displacement behavior during fiber pullout can be described as constant slip, slip softening, or slip hardening (Fig. 2) [49].

2.6. Statistical analysis

One-way ANOVA tested the effect of plastic type on contact angle and mineral deposition on fiber surfaces. Two-factor ANOVA tested the effects of plastic type, biomineralization treatment, and the interaction of these factors on measures from fiber pullout testing. Significance was defined a priori at p<0.05. In the case of main effects with more than two levels or in the case of significant interactions, a Tukey test was performed to discern simple effects. A Tukey test is a post-hoc procedure that allows for multiple pairwise comparisons while maintaining the overall family-wise error at $\alpha=0.05$. ANOVA models satisfied assumptions of residual normality and equal variance. The response was transformed, if necessary, to satisfy these assumptions. All analyses were performed using Minitab (v.19).

3. Results

3.1. Fiber surface and biomineral coating characterization

The MICP treatment was successful in depositing biomineral on all plastic types (Table 2, Fig. 3). The amount of mineral per fiber and the ratio of mineral weight per gram of plastic did not significantly differ by plastic type. XRD diffractograms (Fig. 4) demonstrate that the coating consists of mainly calcite and small amounts of vaterite. FESEM images suggest that the biomineral is deposited in patches on the surface of each plastic type. EDS mapping confirms that these surface deposits are calcium-rich, consistent with CaCO₃ (Fig. 3F).

Table 2 Mineral precipitation and surface properties of plastic fibers. Measurements are reported as mean \pm standard deviation.

| Plastic Type | Mineral precipitated (g) per fiber | g CaCO ₃ /g fiber | Contact Angle of untreated fiber (°) |
|--|--|--|--|
| 3 PVC 4 LDPE 5 PP 6 PS 7 ABS | $\begin{array}{c} 0.04\pm0.01\\ 0.03\pm0.01\\ 0.04\pm0.01\\ 0.04\pm0.01\\ 0.04\pm0.01\\ 0.04\pm0.01\\ \end{array}$ | $\begin{array}{c} 0.24 \pm 0.05 \\ 0.28 \pm 0.07 \\ 0.34 \pm 0.11 \\ 0.29 \pm 0.07 \\ 0.35 \pm 0.10 \end{array}$ | 87.66 ± 1.86 98.13 ± 2.14 98.94 ± 1.36 96.44 ± 2.38 82.46 ± 5.54 |

Video contact angle (VCA) measurements identified that untreated ABS and PVC were hydrophilic as their contact angles were less than 90° . PVC was not hydrophobic (VCA of 87.66°) but was near the hydrophobic threshold of 90° while ABS was more hydrophilic (VCA 82.46°) than PVC. LDPE, PP, and PS were all hydrophobic, with contact angles greater than 90° (Table 2). These VCA measurements are in general agreement with commonly reported contact angles [50–52]. However, due to the material being recycled and formed into fibers, there may be geometry and surface roughness characteristics that result in varying contact angles from those previously reported.

3.2. Plastic type, not MICP treatment, is the main influence of bond strength

3.2.1. Fiber pullout behavior

The pullout curves from the SFPO tests are shown in Fig. 5. The pullout curves demonstrate that, in general, plastic type and not MICP treatment determine fiber pullout behavior. The dominant pullout behavior for all treated and non-treated plastic types was slip softening, as evidenced by the continual decrease of the load in the debonding region. PS snapped before fiber pullout began and no pullout curves could be generated. The max loads during single fiber pullout tests are given in Table 3.

3.2.2. 7-day SFPO results

From two-factor ANOVA, there was a significant interaction between plastic type and biomineral treatment on the interfacial bond strength (τ_a) and chemical bond energy (G_d) (p < 0.05 for both). Post-hoc Tukey comparisons revealed that τ_a and G_d were higher for untreated PVC compared with treated PVC. For all other plastics, untreated and treated fibers did not differ for either τ_a nor G_d . However, these measures showed differences by plastic type (Fig. 6). ABS had much higher interfacial bond strength and chemical bond energy than for other plastics (Fig. 6C). Grouping information from Tukey tests is shown in Table S3.

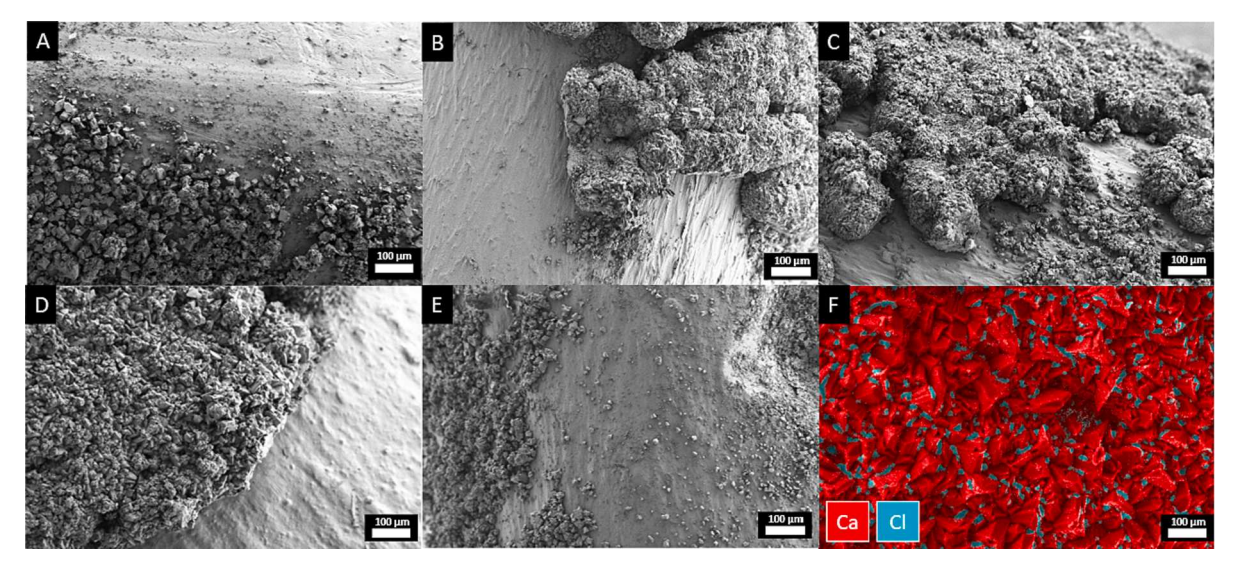


Fig. 3. FESEM images of microbially-induced calcium carbonate precipitation coatings on (A) PVC, (B) LDPE, (C), PP, (D), PS, and (E) ABS fibers at approximately 350× magnification. (F) EDS mapping of the calcium carbonate biomineral coating for treated PVC.

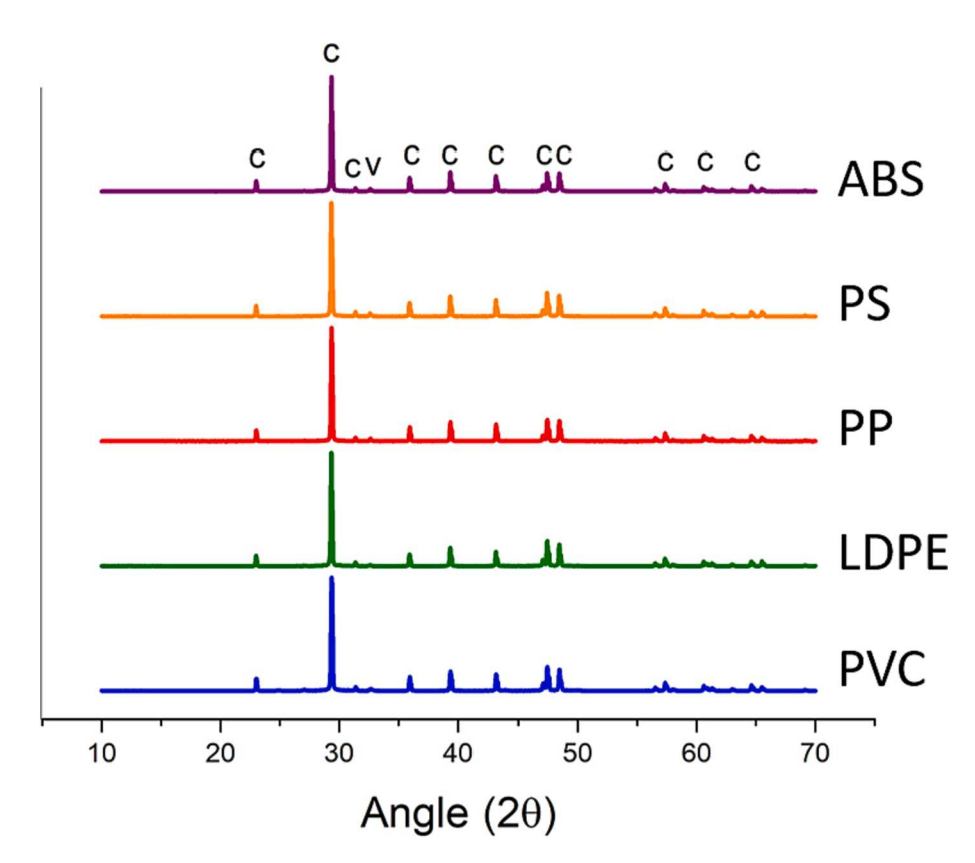


Fig. 4. XRD diffractograms of biomineral deposited on plastic types 3–7. Diffractograms reveal that calcite (c) is the major mineral formed and that vaterite (v) is a minor phase.

Plastic type significantly affected frictional bond strength (τ_b) and work to pullout. Biomineral treatment and the interaction between plastic type and biomineral treatment were not significant. Post-hoc comparisons showed that the order from highest to lowest values for τ_b was ABS, PVC, PP, and LDPE, respectively (Fig. 6B). ABS had the largest work to pullout, followed by PVC and PP sharing the same mean, and LDPE had the lowest work to pullout (Fig. 6D).

3.2.3. 28-day SFPO results

For all plastic types, MICP treatment significantly lowered the mean

values of τ_a and τ_b at 28 days (Fig. 7A and B). Post-hoc comparisons of plastic type showed that at 28 days, ABS had the highest mean values for both τ_a and τ_b followed by PVC, PP, and LDPE respectively (Table S4).

Plastic type significantly affected G_d and work to pullout. MICP treatment did not significantly affect these bonding characteristics. Tukey testing shows that ABS had the largest G_d , followed by PP and LDPE with similar means to each other, and, finally by PVC with the lowest value (Fig. 7C). Tukey tests showed that ABS and PVC shared the highest mean work to pullout. Work to pullout was lower for PP than ABS, but PP and PVC were not significantly different. LDPE had the

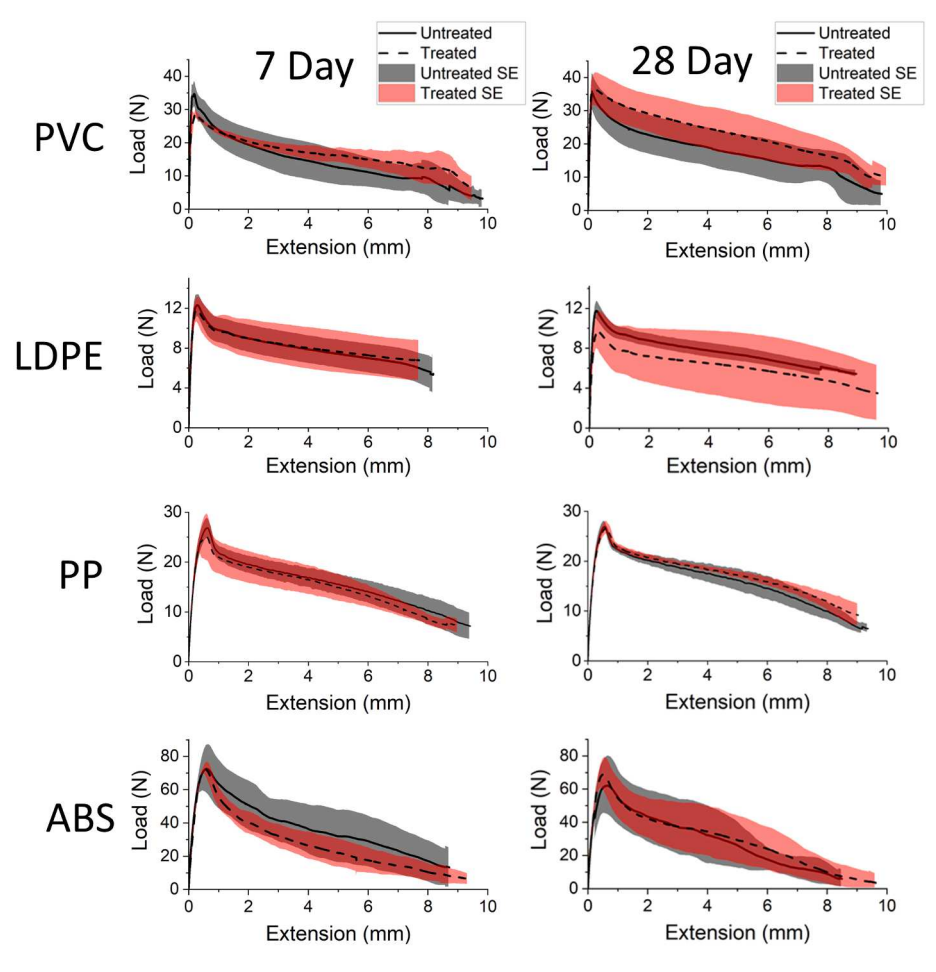


Fig. 5. Single fiber pullout curves for PVC (A), LDPE (B), PP (C), and ABS (D). The shaded region surrounding the bolded mean line is the standard deviation (SD) from each pullout test.

Table 3 Max load (N) experienced during single fiber pullout testing at 7d and 28d timepoints. All data reported as mean \pm standard deviation.

| Plastic Type | 7d | | 28d | |
|--------------|-----------------|----------------|------------------|------------------|
| | Untreated | Treated | Untreated | Treated |
| #3 PVC | 36.17 ± 3.85 | 29.23 ± 1.56 | 36.28 ± 6.52 | 37.48 ± 5.27 |
| #4 LDPE | 12.41 ± 1.17 | 11.93 ± 1.32 | 11.84 ± 0.96 | 9.85 ± 1.92 |
| #5 PP | 27.06 ± 2.20 | 26.11 ± 3.20 | 27.08 ± 1.13 | 26.76 ± 1.52 |
| #6 PS | 45.65 ± 2.44 | 44.02 ± 2.35 | 46.96 ± 1.09 | 43.96 ± 2.62 |
| #7 ABS | 75.07 ± 12.82 | 73.78 ± 3.26 | 65.66 ± 17.62 | 69.68 ± 9.93 |

lowest work to pullout (Fig. 7D, Table S4).

3.2.4. Post SFPO test surface

FESEM imaging was performed after SFPO testing for MICP treated and untreated plastic fibers (Fig. 8). From these images, no evidence of surface abrasions or peeling of plastic surface were found for any plastic type. Post imaging revealed that nearly all the biomineral had been removed from the fiber. Structures that appeared to be hydrated cement and biomineral were occasionally seen on the fiber surfaces (Fig. S2).

4. Discussion

The purpose of this research was to determine the bonding characteristics between low-value plastics and the cement mortar interface. It also served to test the hypothesis that MICP treatment would increase the bond strength between PVC and cement mortar. While PVC, LDPE,

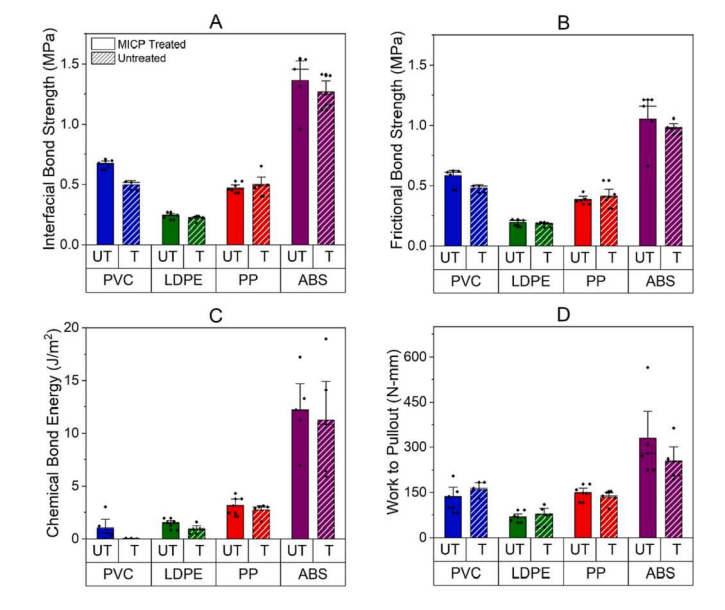


Fig. 6. (A) Interfacial bond strength, (B) frictional bond strength, (C) chemical bond energy, and (D) work to pullout for single fiber pullout testing at 7 days of curing. Error bars indicate one standard deviation. UT = untreated, T = MICP treated. n = 5 for LDPE, PP, ABS, PVC (UT). n = 3 for PVC (T).

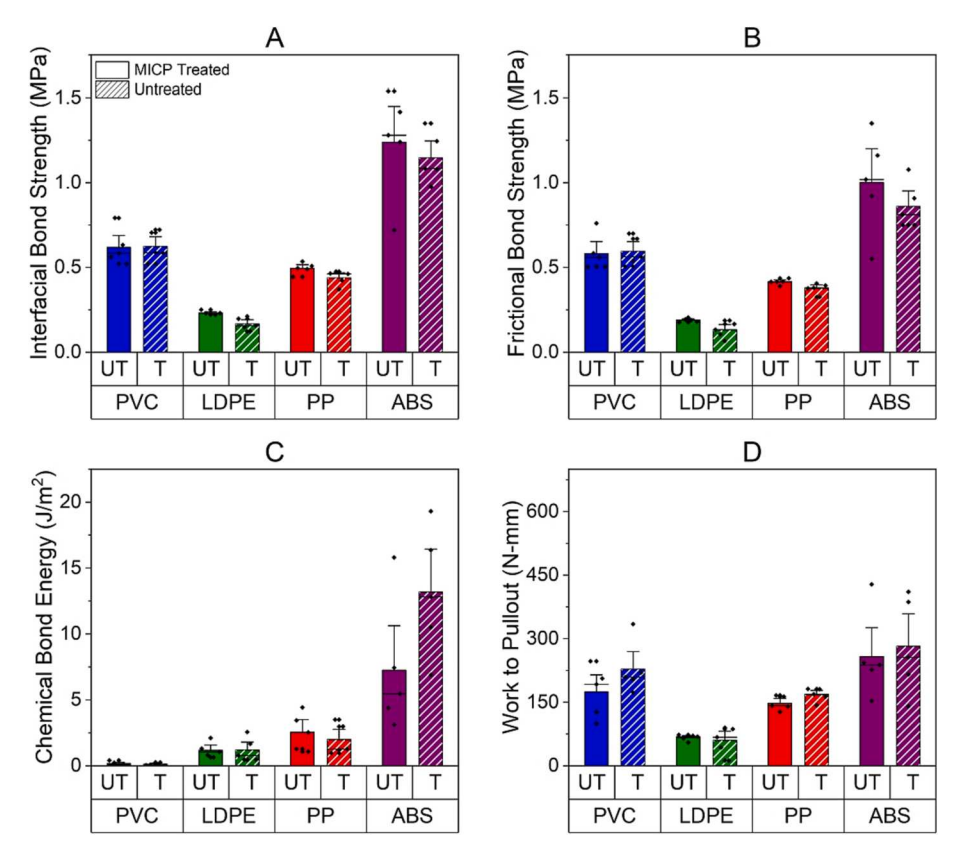


Fig. 7. (A) Interfacial bond strength, (B) frictional bond strength, (C) chemical bond energy, and (D) work to pullout for single fiber pullout testing at 28 days of curing. Error bars indicate one standard deviation. UT = untreated, T = MICP treated. n = 5 for each plastic type.

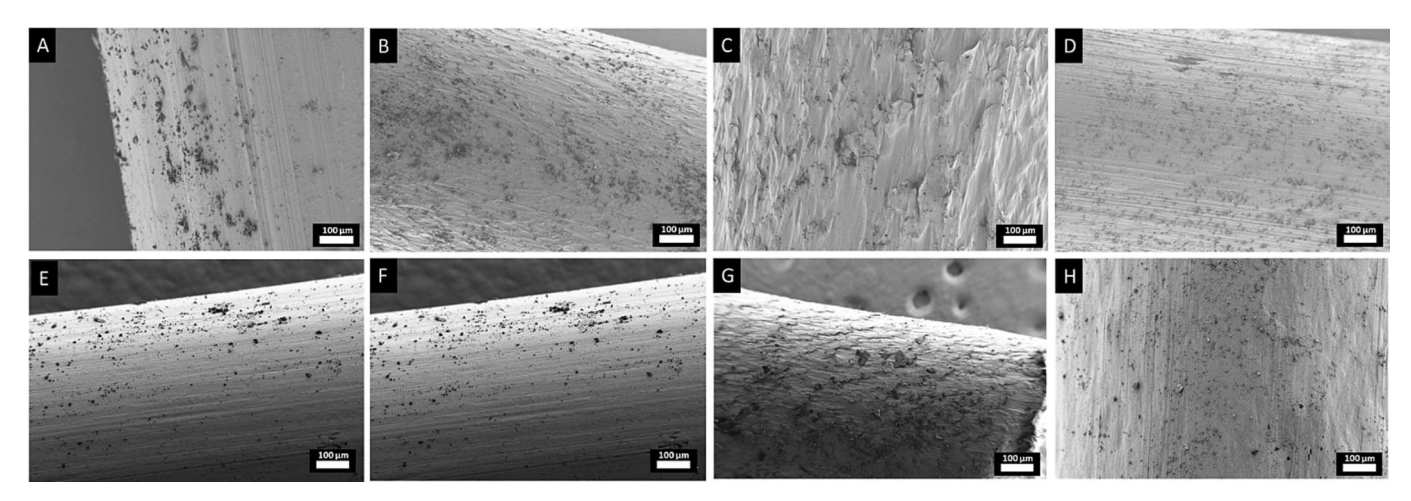


Fig. 8. Post-pullout FESEM images of A-D untreated and E-H treated PVC, LDPE, PP, and ABS embedded sections, respectively.

PS, and ABS are common low-value plastics that may be attractive for use in cementitious materials, their bonding properties to the cement matrix are not well-understood. Furthermore, while reports have shown that coating PP with CaCO₃ via MICP [34] or other methods [35] increased the interfacial bond strength with cement mortar, it is not known whether MICP treatment improves the bond strength for other low-value plastics. In addition, the feasibility of biomineralization on PVC, LDPE, PS, and ABS was largely unknow and therefore investigated in this study. This work aimed to address these gaps by determining the interfacial bond strength (τ_a), frictional bond strength (τ_b), chemical bond energy (G_d), and work to pullout for types 3–7 plastics with and without MICP treatment.

Differences in frictional strength and chemical bond energy

contributed to the overall variation in bond strengths between plastic types. ABS had the strongest values for all measures, including τ_a , τ_b , G_d , and work to pullout. PVC, PP, and LDPE had progressively lower τ_a , τ_b , and work to pullout. G_d followed a different pattern. PVC had the lowest value, followed by similar LDPE and PP, and finally ABS with the highest G_d . The determinants of bond strength between the plastic fibers and the cement matrix may include fiber tensile strength, roughness, and surface energy [23,39,49]. It was found that the variation in τ_a between fiber types did not correspond with variation in tensile modulus (Table 1). Specifically, PVC and ABS had the highest tensile moduli but had opposite bonding characteristics. For example, PVC had an approximately 50% decrease in τ_a compared to ABS at both 7d and 28d time points. Fiber roughness, as estimated from FESEM images, also does not

seem to drive the results. PP fibers appear to have the highest roughness but have midrange bond strengths compared with the other plastics investigated (Fig. 8). The water contact angle, which is related to the surface energy, had good correspondence with chemical bond energy characteristics. ABS had the strongest G_d and was most hydrophilic. The other plastics either demonstrated hydrophobicity (LDPE, PP, PS) or weak hydrophilicity (PVC) measured by their contact angles with water (Table 2). The PS fibers broke before single fiber pullout testing was complete (tensile stress was within 98% of the PS ultimate tensile strength, Table S2), hence PS is not included in the discussion of fiber surface characteristics or interfacial bonding parameters.

ABS had much stronger bond strengths with cement mortar, driven by higher G_d and τ_b compared with PVC, LDPE, and PP. These data are in good correspondence with the differences in compressive strength for PRM containing 5 wt% untreated plastic fibers reported in prior work by Kane and coauthors [16]. In a prior study conducted by the authors, it was found that 5 wt% ABS reinforced mortar without MICP treatment had higher compressive strength than PRMs including untreated LDPE, PVC, PS, or PP fibers [16]. Others also report high strengths of cementitious composites that utilize ABS. For instance, mortar prepared with a 5% replacement of sand by ABS had higher compressive strength at 28 days than control mortar [53]. Together, these results suggest that ABS may be a better choice for engineering higher strength PRCs than other low-value recyclable plastics.

Contrary to the initial hypothesis, the MICP biomineral treatment used in this work did not improve bond strengths. In one case (PVC at the 7d time point), MICP treatment reduced bond strengths and chemical bond energy. For all other plastics at both time points, MICP treatment did not affect measures of the interfacial bond. These findings are in contrast with other reports where the interfacial bonding properties of PP were improved with MICP [34] or abiotic nano-CaCO3 treatments [35]. However, it is important to note that the measured bond strength parameters for PP are in good correspondence with a previous study that used similar embedment lengths and pullout rates without any treatments [40]. The differences in results between the present study and these prior investigations may indicate that the method of biomineral coating influences how it affects the bond strength. Hao et al. [34] reported that a 0.094 CaCO₃ g/g fiber coating improved interfacial bonding for PP and cement matrix more than for either $0.026\ CaCO_3\ g/g$ fiber or $0.374\ CaCO_3\ g/g$ fiber coatings. In the present study, the ratio of CaCO₃ g/g fiber was well above 0.094 for all plastic types (Table 2). The thick, brittle coating (Fig. 3) may dissociate from the fibers and therefore not contribute to bonding with the cement matrix. Adhesives may also improve the bonding of CaCO₃ to plastic. A paraffin wax coating used to adhere the abiotic nano-CaCO3 by Feng and coworkers resulted in improved bond strength of PP to cement mortar [35]. Therefore, in some contexts, CaCO₃ coatings deposited by MICP or other methods, may have the potential to improve plastic bonding strength to cement.

While MICP did not improve bonding parameters in this study, it was observed in the author's prior investigation that the same MICP treatment improved PRM composite strength for 5 wt% PVC and for a mixture of types 3–7 plastics [16]. These data indicate that the biomineral likely influences other factors which lead to the increase in mechanical performance of PRM but not the bond strength. MICP treatment may improve cement hydration around the interfacial transition zone between treated fiber and mortar matrix or affect composite porosity. The influence of MICP treatment on these other factors would benefit from additional investigation.

This study had several limitations. 3D printer filament was utilized because the uniform filament size simplified SFPO testing and allowed comparisons between plastic types. These filament dimensions are not ideal for PRM reinforcements. The sample size for PVC 7 day treated samples was reduced to n=3 from n=5 because of a load frame error. Finally, determining the impact of MICP treatment and plastic type on PRM hydration, porosity, and durability were outside of the scope of the

present study.

5. Conclusions

This study compared interfacial bond strength characteristics from single fiber pullout tests for MICP treated and untreated plastic types 3-7 embedded in OPC mortar. Plastic type had a large influence on measures of bond strength. ABS had superior interfacial bond strength over PP, PVC, and LDPE plastics. The variation in bond strengths between plastic types more closely corresponded with the surface energies of the fibers as opposed to surface roughness or fiber tensile strength. MICP treatment did not significantly influence most interfacial bond strengths, frictional bond strengths, chemical bond energies, or work to pullout measures at either 7d or 28d of curing. In some cases, as for PVC at 7d of curing, MICP significantly lowered measures of bond strength. The reason the MICP treatment did not improve the bond strength in this work, is likely attributed to the thick and inconsistent coverage of biomineral over the fiber surface. The results of this work demonstrate that the beneficial influence of MICP on PRM compressive strength is not simply determined by an increase in bond strength. Furthermore, these results demonstrate that plastic reinforcements can have quite different bonding strengths with cement, which may be useful in the design of PRM and PRC. In particular, the high bond strengths and chemical bond energies of ABS make this plastic an attractive candidate for PRM and PRC applications.

CRediT authorship contribution statement

Michael Espinal: Conceptualization, Data curation, Formal analysis, Funding acquisition, Investigation, Methodology, Writing – original draft, Writing – review & editing. Seth Kane: Data curation, Methodology, Writing – review & editing. Cecily Ryan: Conceptualization, Funding acquisition, Writing – review & editing. Adrienne Phillips: Conceptualization, Funding acquisition, Writing – review & editing. Chelsea Heveran: Conceptualization, Funding acquisition, Methodology, Writing – original draft, Writing – review & editing, Supervision.

Declaration of Competing Interest

The authors declare that they have no known competing financial interests or personal relationships that could have appeared to influence the work reported in this paper.

Data availability

Data will be made available on request.

Acknowledgements

The authors would like to thank the Montana Nanotechnology Facility, Montana State University Undergraduate Scholars Program, and the McNair Scholars Program (U.S.Dept. of Education TRIO McNair Scholars Program, grant #P217A180134) for funding M.E. This work was performed in part at the Montana Nanotechnology Facility, a member of the National Nanotechnology Coordinated Infrastructure (NNCI), which is supported by the National Science Foundation (Grant# ECCS-2025391). S.K.'s contribution was funded by the Environmental Research and Education Foundation Ph.D. scholarship. This material is based upon work supported by the National Science Foundation, under grant CMMI 2036867. Any opinions, findings, and conclusions or recommendations expressed in this material are those of the authors and do not necessarily reflect the views of the National Science Foundation. We also thank Dr. Stephen Sofie, Dr. Kirsten Matteson, and Dr. Michael Berry for access to equipment as well as advice. Thank you to Dr. Sara Maccagnano-Zachar for assistance with XRD and FESEM analysis and

interpretation, and Jorge Osio-Norgaard and Dr. Roberta Amendola for their technical advice on this work.

Appendix A. Supplementary data

Supplementary data to this article can be found online at https://doi.org/10.1016/j.conbuildmat.2022.129331.

References

- A. Naqi, J.G. Jang, Recent progress in green cement technology utilizing lowcarbon emission fuels and raw materials: a review, Sustainability (Switzerland) 11 (2019) 537, https://doi.org/10.3390/su11020537.
- [2] R.M. Andrew, Global CO 2 emissions from cement production, Earth Syst. Sci. Data 10 (2018) 195–217, https://doi.org/10.5194/essd-10-195-2018.
- [3] N. Makul, Modern sustainable cement and concrete composites: REVIEW of current status, challenges and guidelines, Sustain. Mater. Technol. 25 (2020) e00155.
- [4] R. Geyer, J.R. Jambeck, K.L. Law, Production, use, and fate of all plastics ever made, Sci. Adv. 3 (2017), https://doi.org/10.1126/SCIADV.1700782.
- [5] R. Geyer, Production, use, and fate of synthetic polymers, in, Plast. Waste Recycl. (2020) 13–32, https://doi.org/10.1016/b978-0-12-817880-5.00002-5.
- [6] B.S. Al-Tulaian, M.J. Al-Shannag, A.R. Al-Hozaimy, Recycled plastic waste fibers for reinforcing Portland cement mortar, Constr. Build. Mater. 127 (2016) 102–110, https://doi.org/10.1016/j.conbuildmat.2016.09.131.
- [7] N. Pešić, S. Živanović, R. Garcia, P. Papastergiou, Mechanical properties of concrete reinforced with recycled HDPE plastic fibres, Constr. Build. Mater. 115 (2016) 362–370, https://doi.org/10.1016/j.conbuildmat.2016.04.050.
- [8] S. Gupta, H.W. Kua, S.Y. Tan Cynthia, Use of biochar-coated polypropylene fibers for carbon sequestration and physical improvement of mortar, Cem. Concr. Compos. 83 (2017) 171–187, https://doi.org/10.1016/J. CFMCONCOMP.2017.07.012.
- [9] N. Saikia, J. De Brito, Use of plastic waste as aggregate in cement mortar and concrete preparation: a review, Constr. Build. Mater. 34 (2012) 385–401, https:// doi.org/10.1016/j.conbuildmat.2012.02.066.
- [10] N. Saikia, J. de Brito, Mechanical properties and abrasion behaviour of concrete containing shredded PET bottle waste as a partial substitution of natural aggregate, Constr. Build. Mater. 52 (2014) 236–244, https://doi.org/10.1016/j. conbuildmat 2013 11 049
- [11] O.Y. Marzouk, R.M. Dheilly, M. Queneudec, Valorization of post-consumer waste plastic in cementitious concrete composites, Waste Manage. 27 (2007) 310–318, https://doi.org/10.1016/j.wasman.2006.03.012.
- [12] N. Haghighatnejad, S.Y. Mousavi, S.J. Khaleghi, A. Tabarsa, S. Yousefi, Properties of recycled PVC aggregate concrete under different curing conditions, Constr. Build. Mater. 126 (2016) 943–950, https://doi.org/10.1016/j. conbuildmat.2016.09.047.
- [13] S.C. Kou, G. Lee, C.S. Poon, W.L. Lai, Properties of lightweight aggregate concrete prepared with PVC granules derived from scraped PVC pipes, Waste Manage. 29 (2009) 621–628, https://doi.org/10.1016/j.wasman.2008.06.014.
- [14] M.J. Islam, M.S. Meherier, A.K.M.R. Islam, Effects of waste PET as coarse aggregate on the fresh and harden properties of concrete, Constr. Build. Mater. 125 (2016) 946–951, https://doi.org/10.1016/j.conbuildmat.2016.08.128.
- [15] R. Wang, C. Meyer, Performance of cement mortar made with recycled high impact polystyrene, Cem. Conc. Compo. 34 (2012) 975–981, https://doi.org/10.1016/j. cemconcomp.2012.06.014.
- [16] S. Kane, A. Thane, M. Espinal, K. Lunday, H. Armağan, A. Phillips, C. Heveran, C. Ryan, Biomineralization of plastic waste to improve the strength of plasticreinforced cement mortar, Materials 14 (2021) 1949, https://doi.org/10.3390/ mal4081949
- [17] R. Sharma, P.P. Bansal, Use of different forms of waste plastic in concrete a review, J. Cleaner Prod. 112 (2016) 473–482, https://doi.org/10.1016/j. iclepro.2015.08.042.
- [18] A. Babafemi, B. Šavija, S. Paul, V. Anggraini, Engineering properties of concrete with waste recycled plastic: a review, Sustainability (Switzerland) 10 (11) (2018) 3875.
- [19] A.A. Ramezanianpour, M. Esmaeili, S.A. Ghahari, M.H. Najafi, Laboratory study on the effect of polypropylene fiber on durability, and physical and mechanical characteristic of concrete for application in sleepers, Constr. Build. Mater. 44 (2013) 411–418, https://doi.org/10.1016/j.conbuildmat.2013.02.076.
- [20] N.L. Lovata, M.F. Fahmy, Interfacial bond study of a chemically treated polypropylene fibre-reinforced concrete, Constr. Build. Mater. 1 (1987) 83–87, https://doi.org/10.1016/0950-0618(87)90004-3.
- [21] A. Peled, H. Guttman, A. Bentur, Treatments of polypropylene fibres to optimize their reinforcing efficiency in cement composites, Cem. Concr. Compos. 14 (1992) 277–285, https://doi.org/10.1016/0958-9465(92)90026-R.
- [22] A.M. López-Buendía, M.D. Romero-Sánchez, V. Climent, C. Guillem, Surface treated polypropylene (PP) fibres for reinforced concrete, Cem. Concr. Res. 54 (2013) 29–35, https://doi.org/10.1016/j.cemconres.2013.08.004.
- [23] L. Akand, M. Yang, X. Wang, Effectiveness of chemical treatment on polypropylene fibers as reinforcement in pervious concrete, Constr. Build. Mater. 163 (2018) 32–39, https://doi.org/10.1016/j.conbuildmat.2017.12.068.
- [24] S. Singh, A. Shukla, R. Brown, Pullout behavior of polypropylene fibers from cementitious matrix, Cem. Concr. Res. 34 (2004) 1919–1925, https://doi.org/ 10.1016/j.cemconres.2004.02.014.

- [25] C. Zhang, V.S. Gopalaratnam, H.K. Yasuda, Plasma treatment of polymeric fibers for improved performance in cement matrices, J. Appl. Polym. Sci. 76 (2000) 1985–1996, https://doi.org/10.1002/(SICI)1097-4628(20000628)76:14<1985:: AID-APP1>3.0.CO:2-G.
- [26] V.C. Li, H.C. Wu, Y.W. Chan, Effect of plasma treatment of polyethylene fibers on interface and cementitious composite properties, J. Am. Ceram. Soc. 79 (1996) 700–704, https://doi.org/10.1111/j.1151-2916.1996.tb07932.x.
- [27] H. Wu, V.C. Li, Basic Interfacial Characteristic of Polyethylene Fiber/Cement Composites and its Modification by Plasma, Proc., 5th International Symposium on Brittle Matrix Composites. (BMC-5). (1997) 14–23. http://hdl.handle.net/ 2027.42/84756.
- [28] B. Felekoglu, K. Tosun, B. Baradan, A comparative study on the flexural performance of plasma treated polypropylene fiber reinforced cementitious composites, J. Mater. Process. Technol. 209 (2009) 5133–5144, https://doi.org/ 10.1016/j.jmatprotec.2009.02.015.
- [29] R. Hlůžek, J. Trejbal, V. Nežerka, P. Demo, Z. Prošek, P. Tesárek, Improvement of bonding between synthetic fibers and a cementitious matrix using recycled concrete powder and plasma treatment: from a single fiber to FRC, Eur. J. Environ. Civil Eng. 26 (9) (2022) 3880–3897.
- [30] P. di Maida, E. Radi, C. Sciancalepore, F. Bondioli, Pullout behavior of polypropylene macro-synthetic fibers treated with nano-silica, Constr. Build. Mater. 82 (2015) 39–44, https://doi.org/10.1016/J.CONBUILDMAT.2015.02.047.
- [31] C. Signorini, A. Sola, B. Malchiodi, A. Nobili, A. Gatto, Failure mechanism of silica coated polypropylene fibres for fibre reinforced concrete (FRC), Constr. Build. Mater. 236 (2020) 117549.
- [32] F.U.A. Shaikh, Y. Shafaei, P.K. Sarker, Effect of nano and micro-silica on bond behaviour of steel and polypropylene fibres in high volume fly ash mortar, Constr. Build. Mater. 115 (2016) 690–698, https://doi.org/10.1016/j. conbuildmat.2016.04.090.
- [33] W. Zhang, X. Zou, F. Wei, H. Wang, G. Zhang, Y. Huang, Y. Zhang, Grafting SiO2 nanoparticles on polyvinyl alcohol fibers to enhance the interfacial bonding strength with cement, Compos. B Eng. 162 (2019) 500–507, https://doi.org/10.1016/j.compositesb.2019.01.034.
- [34] Y. Hao, L. Cheng, H. Hao, M.A. Shahin, Enhancing fiber/matrix bonding in polypropylene fiber reinforced cementitious composites by microbially induced calcite precipitation pre-treatment, Cem. Concr. Compos. 88 (2018) 1–7, https:// doi.org/10.1016/j.cemconcomp.2018.01.001.
- [35] J. Feng, F. Yang, S. Qian, Improving the bond between polypropylene fiber and cement matrix by nano calcium carbonate modification, Constr. Build. Mater. 269 (2020), 121249, https://doi.org/10.1016/j.conbuildmat.2020.121249.
- [36] W. de Muynck, N. de Belie, W. Verstraete, Microbial carbonate precipitation in construction materials: a review, Ecol. Eng. 36 (2010) 118–136, https://doi.org/ 10.1016/j.ecoleng.2009.02.006.
- [37] A.J. Phillips, R. Gerlach, E. Lauchnor, A.C. Mitchell, A.B. Cunningham, L. Spangler, Engineered applications of ureolytic biomineralization: a review, Biofouling 29 (2013) 715–733, https://doi.org/10.1080/08927014.2013.796550.
- [38] E. Wölfel, C. Scheffler, I. Curosu, V. Mechtcherine, Single fibre pull-out tests of polypropylene and glass fibres in cement-based matrices at high loading rates, ECCM 2018 – 18th European Conference on Composite Materials (2020) 24–28.
- [39] E. Wölfel, H. Brünig, I. Curosu, V. Mechtcherine, C. Scheffler, Dynamic single-fiber pull-out of polypropylene fibers produced with different mechanical and surface properties for concrete reinforcement, Materials 14 (2021) 1–20, https://doi.org/ 10.3390/MA14040722
- [40] D.L. Naik, A. Sharma, R.R. Chada, R. Kiran, T. Sirotiak, Modified pullout test for indirect characterization of natural fiber and cementitious matrix interface properties, Constr. Build. Mater. 208 (2019) 381–393, https://doi.org/10.1016/j. conbuildmat.2019.03.021.
- [41] H.R. Pakravan, M. Jamshidi, M. Latifi, M.M. Chehimi, Polymeric fibre adhesion to the cementitious matrix related to the fibres type, water to cement ratio and curing time, Int. J. Adhes. Adhes. 35 (2012) 102–107, https://doi.org/10.1016/j. ijadhadh.2012.02.006.
- [42] Z. Lin, V.C. Li, Crack bridging in fiber reinforced cementitious composites with slip-hardening interfaces, J. Mech. Phys. Solids 45 (1997) 763–787, https://doi.org/10.1016/S0022-5096(96)00095-6.
- [43] Y. Wang, V.C. Li, S. Backer, Modelling of fibre pull-out from a cement matrix, Int. J. Cem. Compos. Lightweight Conc. 10 (1988) 143–149, https://doi.org/10.1016/0262-5075(88)90002-4.
- [44] A. Bhutta, M. Farooq, C. Zanotti, N. Banthia, Pull-out behavior of different fibers in geopolymer mortars: Effects of alkaline solution concentration and curing, Mater. Struct./Materiaux et Constructions. 50 (2017) 1–13, https://doi.org/10.1617/ s11527-016-0889-2.
- [45] ASTM C305, Standard Practice for Mechanical Mixing of Hydraulic Cement Pastes and Mortars of Plastic Consistency, ASTM Lnternational. (2011) 1–3. https://doi. org/10.1520/C0305-14.2.
- [46] ASTM, Standard Practice for Making and Curing Concrete Test Specimens in the Laboratory, (2007) 1–8. https://doi.org/10.1520/C0192.
- [47] T. Kanda, V.C. Li, Interface property and apparent strength of high-strength hydrophilic fiber in cement matrix, J. Mater. Civ. Eng. 10 (1998) 5–13, https://doi. org/10.1061/(ASCE)0899-1561(1998)10:1(5).
- [48] Z. Lin, T. Kanda, V.C. Li, On interface property characterization and performance of fiber reinforced cementitious composites, J. Conc.Sci. 1 (1999) 173–184.
- [49] C. Redon, V.C. Li, C. Wu, H. Hoshiro, T. Saito, A. Ogawa, Measuring and modifying interface properties of PVA fibers in ECC matrix, J. Mater. Civ. Eng. 13 (2001) 399–406, https://doi.org/10.1061/(asce)0899-1561(2001)13:6(399).
- [50] D.K. Owens, R.C. Wendt, Estimation of the surface free energy of polymers, J. Appl. Polym. Sci. 13 (1969) 1741–1747, https://doi.org/10.1002/app.1969.070130815.

- [51] L. Magallón Cacho, J.J. Pérez Bueno, Y. Meas Vong, G. Stremsdoerfer, F.J. Espinoza Beltrán, J. Martínez Vega, Novel green process to modify ABS surface before its metallization: optophysic treatment, J. Coat. Technol. Res. 12 (2015) 313–323, https://doi.org/10.1007/s11998-014-9632-5.
- [52] P.F. Rios, H. Dodiuk, S. Kenig, S. McCarthy, A. Dotan, The effect of polymer surface on the wetting and adhesion of liquid systems, J. Adhes. Sci. Technol. 21 (2007) 227–241, https://doi.org/10.1163/156856107780684567.
- [53] G. Kaur, S. Pavia, Physical properties and microstructure of plastic aggregate mortars made with acrylonitrile-butadiene-styrene (ABS), polycarbonate (PC), polyoxymethylene (POM) and ABS/PC blend waste, J. Build. Eng. 31 (2020), 101341, https://doi.org/10.1016/j.jobe.2020.101341.